

Kevlar-like Aramid Polymers from Mixed PET Waste

Lelia Cosimbescu,* Deepika Malhotra, Madhusudhan R. Pallaka, and Marie S. Swita

Cite This: *ACS Omega* 2022, 7, 32026–32037

Read Online

ACCESS |

Metrics & More

Article Recommendations

Supporting Information

ABSTRACT: This work describes the synthetic approaches, spectroscopic and thermal characterization of aramid polymers prepared from waste polyethylene terephthalate (PET) via sustainable and scalable processes. Direct depolymerization of PET with aliphatic diamines under melt conditions resulted in decomposition without substantial formation of any aramid polymer. The Higashi–Ogata methodology or direct polycondensation of terephthalic acid (TPA) derived from PET waste and *p*-phenylenediamine, resulted in oligomerization and formation of aramids with a low degree of polymerization. The highest molecular weight polymers were obtained via the acid chloride of TPA, the traditional method. A proprietary solvent enabled the dissolution of most polymers and subsequent size exclusion chromatography analysis in the same solvent. We emphasize that although the soluble polymer compounds are prepared via the traditional route, they are novel. The apparent molecular weights of the soluble polymers ranged between 10–35 kDa (M_n) and 28–81 kDa (M_w). All analogues were prepared with commercially available diamines and diamine combinations. The obtained solid powders were dissolved in D_2SO_4 and analyzed spectroscopically to qualitatively evaluate the degrees of polymerization, while the solids were characterized via thermogravimetric analysis and differential scanning calorimetry. Many reaction conditions were employed to improve the solution polycondensation reaction, and it was found that addition of pyridine (2 eq) to the NMP reaction medium was crucial in preventing the precipitation of the polymer. Contrary to conventional wisdom, $CaCl_2$ did not play a crucial role in the molecular weight increase of the polymer when oxydianiline was used. Our data indicated that the temperature and absence of $CaCl_2$ provided a boost in molecular weight. Both room temperature and 0 °C reactions generated similar polymers as suggested by nuclear magnetic resonance; however, the cold conditions enhanced gel formation, an important attribute in the future processing of these materials to obtain fibers. All analogues had a high degradation temperature at 5 and 10% weight loss ($T_{5\%}$ and $T_{10\%}$), above 400 °C, along with high percent char values. A glass transition (T_g) was not detected in any of the analogues prepared.



1. INTRODUCTION

With the rising consumption of plastics, the generation of plastic wastes is also increasing rapidly around the world. By 2050, up to 26 billion tons of plastic waste is anticipated to be created, and approximately 50% will be tossed into landfills, leading to grim environmental pollution and inherent loss of petroleum-based carbon contained in these products. The annual global plastic production was estimated to be around 388 Mton in 2019, of which approximately 8% corresponds to the manufacture of polyethylene terephthalate (PET).^{1,2} In 2019, the consumption of PET was valued at \$43.81 billion and is projected to reach \$68.33 billion by 2023.^{3,4} Mechanical recycling of PET is already adopted; however, chemical contamination and degradation are sources of impurities in the recycling stream. Recycled materials require efficient sorting, separation, and cleaning processes for the production of high-quality recycled polyester. As a result, the recycling rates for colored bottles and films are significantly lower due to the broad range of colors, additives, multilayer structures, labels, and adhesives. This challenge may be overcome by

chemical recycling, which is tolerant to contaminants from mixed-waste streams, allow removal of impurities in the process, and yield quality monomer (terephthalic acid, TPA) feedstocks or other high-end products.

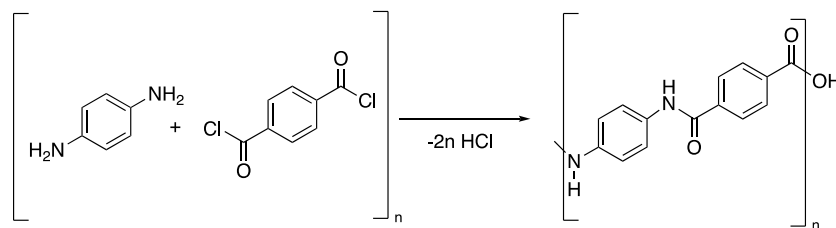
In the context of developing novel ways to valorize PET waste to create high-end products and further a sustainable circular economy, we devised strategies to generate Kevlar-like materials. Kevlar is a commercially available aramid fiber, developed at DuPont while searching for a new lightweight fiber to use for light, but strong, tires.^{5,6} Kevlar is a poly-*para*-phenylene terephthalamide polymer that is prepared by the condensation reaction of *para*-phenylenediamine with terephthaloyl chloride (Scheme 1). The resulting polyamide

Received: May 16, 2022

Accepted: August 10, 2022

Published: August 26, 2022



Scheme 1. Synthesis of Kevlar by the Polymerization of Paraphenylenediamine and Terephthaloyl Chloride⁷

polymer containing aromatics and amide groups has a rigid rod-like structure which translates into a very high tensile strength of the resulting fibers spun from it but also has very poor solubility and processability (referenced above).

On the other hand, carbon fibers have found a wide range of applications in the aerospace, automotive, and consumer industries due to their versatile physical properties. In the past decade, lightweighting of automotive components has gained substantial attention to not only reduce the carbon footprint but also conserve valuable and exhausting resources. Although carbon fibers have a high potential for weight saving of a vehicle body and chassis structures, one primary reason for not using them widely in the current high-volume production vehicles is their high cost. Together with desirable properties, they bring a set of disadvantages such as brittleness and low recyclability. Once the virgin structure is damaged, it needs to be discarded and replaced by a new one which accounts for the higher pricing. Aramid fibers, such as Kevlar, can provide an alternative or potential replacement to carbon fibers by offering superior performance while conserving a high strength-to-weight ratio at a lower cost.⁸

In this work, we combined mixed-waste PET chemical recycling with the synthesis of high-value Kevlar-like aramid polymers. Several strategies were explored to this end, including direct deconstruction of PET with nucleophilic amines, similar to aminolysis, depolymerization of PET to TPA, and subsequent polymerization under melt conditions, Higashi–Ogata condensation, and conventional condensation via a terephthaloyl chloride intermediate. Synthetic considerations and challenges are discussed with each approach. The overarching goal of this work is to develop aramid polymers from recycled PET that can help reduce the current cost barrier limiting the wide application of such components in the automotive industry. Utilizing waste PET as a cheap starting material to produce these polymers will not only be cost-effective but also provide a novel pathway to PET chemical upcycling.

2. METHODS

2.1. Materials. The diamines phenylene diamine (PDA, ortho and para), 4,4'-diaminodiphenyl ether, piperazine, 4,4'-diaminodiphenylmethane, 1,5-diaminonaphthalene, 1,3-propylene diamine, and thionyl chloride were purchased from Aldrich Chemical Company (Milwaukee, WI) or TCI America (Portland, OR) and used as received without further purification. Anhydrous pyridine and *N*-methyl-2-pyrrolidone (NMP) were purchased from Aldrich and used as received. Other common reagents utilized in the synthesis or work up such as sodium hydroxide, concentrated hydrochloric acid, dichloromethane, methanol, acetone, dimethylformamide (DMF), and hexamethylphosphoramide (HMPA) were purchased from Fisher Scientific (Hampton, NH). Powdered,

virgin PET for model reactions was purchased from Goodfellow Corporation (Coraopolis, PA). TPA was obtained from mixed-waste PET, composed of colored, clear, and opaque yellow bottles whose labels and caps were not removed, via basic hydrolysis, and the study is reported in detail elsewhere.⁹

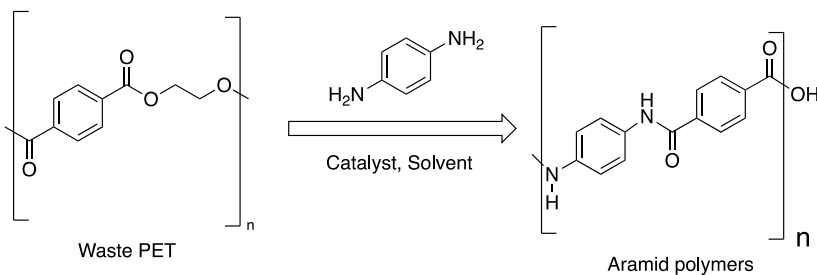
2.2. Synthesis. All chemical manipulations were carried out under standard techniques, under argon or nitrogen atmosphere, in oven-dried glassware, Schlenk transferring techniques, and magnetic stirring. The detailed synthesis of TPA is described in a previous work referenced earlier.

2.2.1. Synthesis of Aramid Polymers via the Higashi–Ogata Method. Several conditions were employed for the direct polymerization of TPA via the Higashi–Ogata method. In one example, a two-neck 250 mL round-bottom flask was charged in the glovebox with 1.039 g of TPA (6.26 mmol, 1 eq), 0.676 g of *para*-phenylenediamine (6.64 mmol, 1.06 eq), 3.75 g of dried CaCl₂ (33.7 mmol), 1.25 g of dried LiCl (29.48 mmol), and 3.6 mL of triphenylphosphite (13.8, 2.04 mmol). The flask containing solids was transferred outside the glovebox, and under a Schlenk line, NMP (60 mL) and pyridine (12.5 mL) were added. The resulting mixture was brought to 100 °C and stirred overnight, during which time the solid started to precipitate out. The next day, the mixture was cooled, and 20 mL of methanol and 50 mL of 1M HCl were added. A very fine beige precipitate formed, which was isolated by filtration. Note: none of the liquid reagents were dried further than as received; filtration of the solid product took hours, despite the small amount of the material.

2.2.2. Terephthaloyl Chloride Method A. The detailed synthesis of one of the aramid polymers is described, and other analogues were prepared following similar protocols. To an oven-dried two-neck round-bottom flask containing a stir bar, 1,4-phenylene diamine (0.9609 g, 4.79 mmol, 1.0 eq) was added in an inert atmosphere inside the glovebox to avoid oxidation of the amine. Also in the glovebox, a separate flask was charged with terephthaloyl chloride (1.023 g, 5.03 mmol, 1.05 eq). Both solids were dissolved in NMP (15 and 22 mL, respectively, transferred under Ar, outside the glovebox). To the solution of diamine in NMP under an argon atmosphere using the Schlenk line, pyridine (0.7591 g, 9.59 mmol, 2.0 eq) was added, followed by the slow addition of the terephthaloyl chloride solution, and the reaction mixture was stirred overnight at room temperature. The reaction mixture which became somewhat viscous was quenched with water (70 mL) to form an off-white precipitate. The solid was filtered, then suspended in acetone or methanol, and stirred for 1 h to remove impurities including NMP, filtered, and dried to yield a pinkish solid (95% yield).

2.2.3. Terephthaloyl Chloride Method B. To an oven-dried two-neck round-bottom flask containing a stir bar, 1,4-phenylene diamine (0.822 g, 7.61 mmol, 1.0 equiv.) and CaCl₂ (1.5 g, ~5% g/mL) were added in an inert atmosphere,

Scheme 2. Direct Depolymerization of PET Waste and Concerted Repolymerization



followed by dissolution in NMP (17 mL). To this solution, pyridine (1.23 g, 15.22 mmol, 2.0 eq) was added, and the flask was cooled to 0 °C. Another flask was charged with terephthaloyl chloride (1.54 g, 7.54 mmol, 1.0 eq) in the glovebox and dissolved in NMP (10 mL). The terephthaloyl chloride solution in NMP was added dropwise to the ice-cooled solution of diamine, and the resulting mixture was stirred for 30 min at 0 °C and at room temperature for 1 h. The reaction mixture became visibly viscous immediately upon the addition of acid chloride. The reaction mixture was quenched with water to precipitate the polymer, which was isolated by filtration. The crude polymer was suspended in water and heated for 2 h at 85 °C to remove salts and NMP. The cleaned polymer was isolated by filtration and rinsed with acetone or methanol to dry.

2.3. Physical Analysis. NMR spectra were obtained with an Agilent-Oxford (Santa Clara, CA, USA) 500 MHz spectrometer at 499.8 MHz (¹H). ¹³C NMR was not performed due to the low concentration of the samples and thus limited utility of the prospective spectra. The chemical shifts are reported in delta (δ) units, parts per million (ppm) up-field from D₂SO₄. Whether small oligomers or higher molecular weight polymers, the aramids were insoluble in all practical deuterated solvents, except sulfuric acid.

2.4. Thermal Analysis. **2.4.1. Differential Scanning Calorimetry.** Differential scanning calorimetry (DSC) experiments were performed using a TA Q2000 calorimeter equipped with a liquid nitrogen cooling system and dry nitrogen as cell gas. The measurement protocol to capture heat flow as a function of temperature involved three steps: 1) heating a sample (~2–5 mg of polymer sealed in 40 μL of aluminum pans) from 2 to 350 °C at a ramp rate of 10 K/min to erase the thermal history, 2) cooling from 350 to 25 °C at 10 K/min to establish a thermal history, and 3) heating the sample back to 350 °C at 10 K/min to capture any possible transitions. The baseline correction for all the measurements was performed using sapphire's heat capacity measurements, and the heat flow and temperature calibrations were performed using the melting transitions of indium and zinc.

2.4.2. Thermogravimetric Analysis. Thermogravimetric analysis (TGA) experiments to evaluate the thermal stability of the respective polymers both in air and N₂ (flow rate of 50 mL/min) were performed using a Mettler Toledo DSC/TGA 1 equipped with a water-cooling system. To capture the mass loss as a function of temperature, a ~4–10 mg polymer sample in 70 μL alumina pans was heated from 25 to 700 °C at a ramp rate of 10 K/min. The temperature calibration for the onset and peak temperatures of the degradation process was performed using the melting transitions of indium and aluminum.

2.4.3. Gel Permeation Chromatography. Samples were analyzed using an Agilent 1260 Infinity II equipped with a refractive index (RI) detector. The sample or standard (100 μL) was injected at a flow rate of 0.7 mL/min solvent at 40 °C. The solvent utilized for solubilizing the polymers as well as the column eluent was NMP additized at 3–5% (w/w) with a proprietary organic compound. Polymethylmethacrylate standards of molecular weights ranging from ~800 to 1.9 million Daltons were prepared at approximate concentrations of 0.75–1.5 mg/mL and were used to generate a calibration curve (Figure S19). Two Jordi Resolve Gel DVB Medium Mixed Bed (300 × 7.8 mm) columns were plumbed in series to achieve separation of the polymethacrylate standards which come in a set of four molecular weights. Agilent gel permeation chromatography/size exclusion chromatography (GPC/SEC) software was used to generate results.

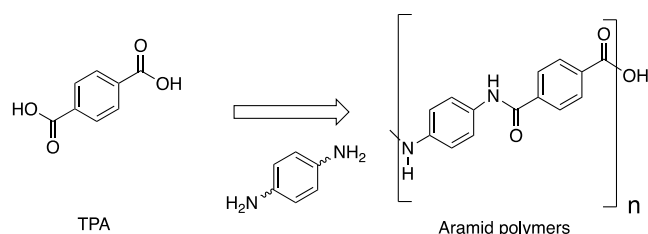
3. RESULTS AND DISCUSSION

3.1. Direct Depolymerization of PET. Our original aramid synthetic strategy involved the direct concerted depolymerization–repolymerization reaction (Scheme 2) via C–O bond cleavage and C–N bond formation. This methodology, if successful, was projected to provide a considerable advantage in the cost of aramid polymers, as the starting material is cheap PET waste. We reported similar aminolysis protocols,¹⁰ but those take place in an excess of amine, which essentially drives the reaction to completion, despite the low PET solubility in that media. In contrast, this reaction requires equivalent amounts of diamine in a suitable solvent. The main challenge is PET insolubility in all non-reactive, relatively inexpensive organic solvents such as DMF, dimethylsulfoxide (DMSO), HMPA, NMP, and dichlorobenzene, thereby making the solution chemistry difficult. The reaction was conducted in dilute NMP at 160 °C with piperazine (0.2 g of PET in 20 mL NMP), a much more nucleophilic amine than an aromatic diamine, without success, in the presence of various catalysts (amines, Zn (OAc)₂). Although PET dissolved at 150 °C, no polymer formed in a significant amount, although about 25% of PET was converted to mono or diamide product. Given the low reactivity with a strong nucleophile, there was no reason to attempt the reaction with phenylene diamine. It is worth noting that piperazine was chosen as a model nucleophilic amine to conduct exploratory chemistry due to its ease of handling in air. Moreover, the reaction is unlikely to go to completion, and separation of insoluble starting materials (unreacted PET) from products (aramid) would be very challenging, if even possible. Furthermore, this approach is not feasible especially for mixed waste due to the presence of impurities which might deactivate the catalyst, thereby hindering the reaction dynamics and interfere with the separation process.

We also investigated the direct *trans*-amidation of pure, fine powder PET in the melt with piperazine, the most nucleophilic of the amines we studied. The starting materials were mixed, ground, and transferred into a 1 mL Swagelok tubular reactor and then loaded into an oven which was held at the desired temperatures from 2 to 4 h. Due to the high melting point of TPA, no change was observed at temperatures below 270 °C. Only when reaching 275–280 °C, depolymerization of PET was obtained with about 70% conversion, with the formation of small char-like fragments soluble in methanol, but without the formation of the desired polymers, or even oligomers. The melting point of PET is ~280 °C, so this result is consistent with increased reactivity in the melt. Temperatures above 300 °C produced substantial decomposition of starting materials with char formation (black insoluble solid). We are currently investigating various catalysts to accomplish the direct depolymerization of PET and repolymerization, albeit a challenging transformation.

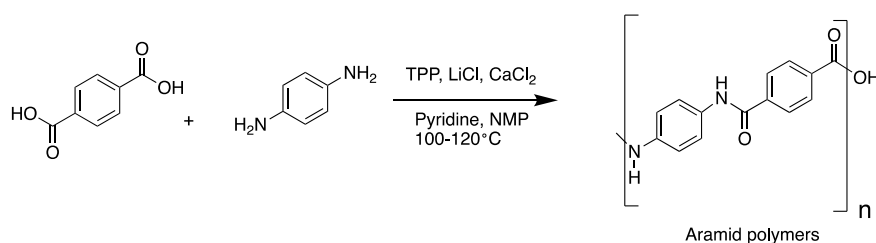
3.2. Aramid Formation through Direct Condensation of TPA. We explored melt polymerization of TPA with various diamines to achieve the direct condensation of the two monomers, approach illustrated in Scheme 3.^{11–13} There are challenges associated with this approach as well, as piperazine and phenylene diamines (para and meta derivatives) sublime around 100 °C while TPA is a very high melting solid (at 300 °C) that starts to slowly sublime around 180 °C. First attempts were conducted in a round-bottom flask, to be able to observe the reaction mixture, but due to the sublimation of the amines which essentially escaped the mixture, we transitioned to a closed Swagelok-type reactor. We attempted several reactions in the presence of various catalysts (ZrCp₂Cl₂, triazabicyclodecene, and Zn(OAc)₂ among others), but similar disappointing results were obtained due to the high melting point of TPA. Temperatures above 300 °C did not produce any polymer, but rather resulted in char formation.

Scheme 3. Synthesis Approach for Aramid Polymers from Terephthalic Acid



Given that the solid or melt chemistry proved challenging, not unexpectedly considering that TPA is a deactivated diacid among other challenges, we decided to investigate the Higashi–Ogata methodology^{14,15} for direct polycondensation

Scheme 4. Direct Polycondensation of TPA and Aromatic Amines



shown in Scheme 4. Typical preparations report distilling starting materials multiple times and involve extreme anhydrous conditions. We conducted the reaction as described in the experimental section, without further drying commercial starting materials, except LiCl and CaCl₂ which were heated under vacuum at 80 °C overnight to remove water. One notable difference between our trials and those reported in the literature is that the polymer always precipitated out in the reaction mixture, instead of gelling and thickening of the reaction medium.

While performing Higashi–Ogata reactions, we noticed that upon mixing TPA with either propylene diamine or piperazine, an immediate precipitate formed, which did not form in the presence of *p*-PDA. The precipitate never dissolved in the reaction medium, and the product yield was low. Puzzled by this finding and suspecting that TPA may form a salt with aliphatic amines, equivalent amounts of TPA and piperazine were mixed in NMP or DMF at room temperature. Indeed, salt formed immediately, confirmed by the dissolution of the product in water, as well as by ¹HNMR in D₂O. It became quite clear that the methodology was limited to weak amines, such as aromatic amines. Furthermore, the reaction with *p*-PDA likely resulted in a low degree of polymerization and incomplete consumption of starting materials indicated by ¹HNMR (terminal repeating units detected). We concluded that the reaction had less than the desirable efficiency, considering the degree of dryness and multiple reagents required, coupled with the difficult filtration of a fine precipitated product.

3.3. Aramid Polymer through Terephthaloyl Chloride. Since acyl chlorides are known to be the most reactive carboxylic acid derivatives, we anticipated that this functional group will improve conversion and generate polyamides with higher degrees of polymerization and higher molecular weights (Scheme 5). Terephthaloyl dichloride was generated in a quantitative yield from the reaction of TPA with thionyl chloride. Although thionyl chloride is not an environmentally desirable reagent, we mitigated its impact by recycling it via distillation. Pyridine is forming the chloride salt in NMP solution, while the amines are consumed in the condensation process. Subsequent reactions utilizing only recycled SOCl₂ did not suffer any drawbacks. It is possible to separate NMP and water via distillation if recovery and recycling of NMP is desired.

Several polymeric analogues were synthesized using the conventional methodology,^{16–21} utilizing different reaction conditions and various diamines and diamine combinations. The objective in studying different amines was twofold: increased solubility of the resulting polymer would prevent its premature precipitation, which essentially terminates the chain growth, and the resulting polymer would be soluble in solvents

Scheme 5. Modified Synthetic Approach for Aramid Polymers from Terephthaloyl Chloride

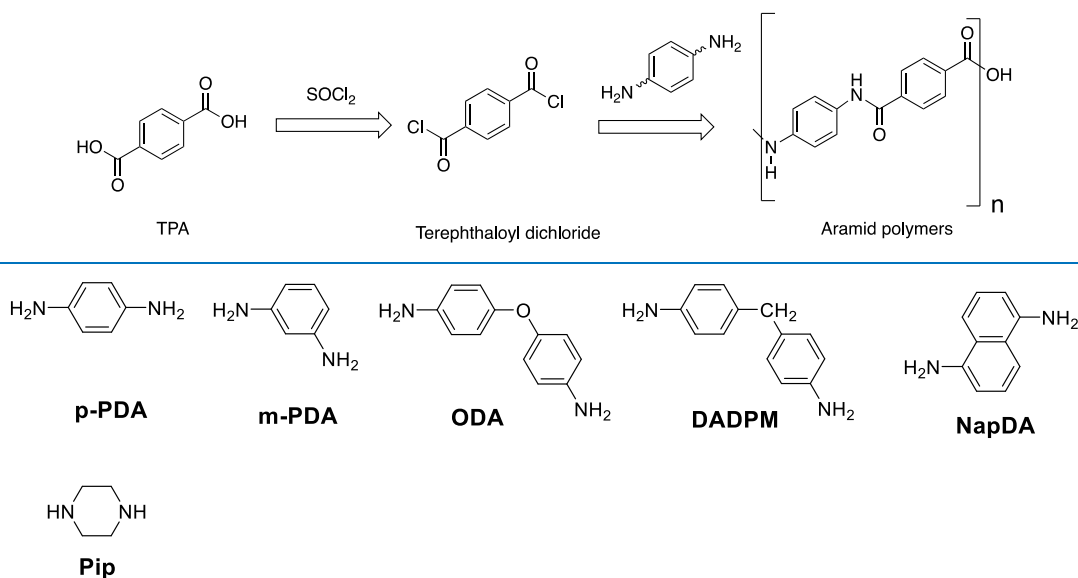


Figure 1. Structures of amines employed in the condensation polymerization: as shown, *p*-PDA = *para*-phenylenediamine, *m*-PDA = *meta*-phenylenediamine, ODA = oxydianiline, DADPM = diaminodiphenyl methane, Pip = piperazine, and NapDA = 1,5-diaminonaphthalene.

Table 1. Amines and Conditions Employed in the Preparation of Aramid Polymers

polymer	method	amine (molar ratio)	additives conc (g/mL)	° C	observations
P1	TPA; higashi	<i>p</i> -PDA: 1	none	100	solid precipitated after 2 h
P2	TPA; higashi	<i>p</i> -PDA: 1	CaCl ₂ (6%) LiCl (2%)	100	solid precipitated after 1 h
P3	TPA chloride	<i>p</i> -PDA: 1	LiCl (2%)	rt	solid precipitated in 5 min
P4	TPA chloride	<i>p</i> -PDA: 1	none	rt	cloudiness, no precipitation
P5	TPA chloride	Pip:1	none	rt	cloudiness, no precipitation
P6	TPA chloride	<i>m</i> -PDA: 1	none	rt	no precipitation
P7	TPA chloride	Pip:1	none	rt	repeat of P5; no precipitation
P8	TPA chloride	<i>m</i> -PDA: 1	none	rt	more concentrated than P6 (~2x); no precipitation
P9	TPA chloride	ODA: 1	none	rt	viscous solution; no precipitation
P10	TPA chloride	NapDA:1	none	rt	precipitation upon addition
P11	TPA chloride	<i>p</i> -PDA:1	CaCl ₂ (5%)	0; rt	viscous solution; no precipitation
P12	TPA chloride	<i>m</i> -PDA:1	CaCl ₂ (5%)	0; rt	viscous solution; no precipitation
P13	TPA chloride	<i>p</i> -PD:ODA; 0.75:0.25	CaCl ₂ (5%)	0; rt	slightly viscous solution; no precipitation
P14	TPA chloride	<i>p</i> -PD:ODA; 0.9:0.1	CaCl ₂ (5%)	0; rt	highly viscous solution; no precipitation
P15	TPA chloride	DADPM	CaCl ₂ (5%)	0; rt	slightly viscous solution; no precipitation

other than sulfuric acid to enable GPC characterization. The poor solubility of these polymers is mainly attributed to the hydrogen bond interactions and Π – Π stacking between the aromatic polymer chains.^{22–25} Figure 1 illustrates the structure of all amines utilized in the synthesis.

Table 1 summarizes the composition of the aramid polymers prepared, along with the additives and reaction conditions utilized (Higashi or terephthaloyl chloride). All condensations with acid TPA chloride utilized equivalent amounts of pyridine (2 eq) as a scavenger for the HCl generated, with one exception. The piperazine reaction was a special case as piperazine itself can be an effective base for the HCl formed. Triethylamine was used as the acid scavenger (4 eq), with the caveat that some piperazine amine would also compete for the acid and subsequently reduce its availability to participate in the polymerization.

The addition of various diamine co-monomers, as well as the investigation of less linear structures than Kevlar polymers prepared with *p*-PDA, targeted a solubility enhancement. The strategy is not new; the solubility of aramid polymers can be

enhanced either by the incorporation of functional groups such as ether or sulfones or by integrating an unsymmetrical non-coplanar structural configuration in the backbone.^{26–28} We chose inexpensive, commercially available diamines to form condensation polymers with TPA. We probed the solubility of the synthesized aramid polymers in DMSO, DMF, NMP, and HMPA, without success; even the most polar and non-linear ODA polymer did not dissolve in common solvents. While sulfuric acid is an acceptable solvent for NMR analysis, it is not suitable for GPC evaluation. It is the reason why most works in this field do not report a molecular weight of the polymers obtained, but an inherent viscosity at best,¹⁹ often measured in H₂SO₄ (conc). Therefore, we investigated various additives in NMP, including common inorganic salts such as CaCl₂ and LiCl. A proprietary NMP mixture containing 3–5% of an organic additive was discovered to provide sufficient solubility for most solid polymers to enable GPC analysis.

It is important to note that preventing the precipitation of the product is critical not only for augmenting the molecular weight of the polymer but also in the future processing of these

materials into fibers, the subject of our future work. Although the generally accepted protocol for high-quality fiber is the isolation and purification of the product, followed by dissolution in sulfuric acid^{29,30} or ionization in the presence of base,³¹ drawing fiber directly from the reaction mixture may provide a cost benefit, if molecular alignment is achieved through shear.

3.4. Spectral Characterization of Aramid Polymers.

All polymers were analyzed by NMR to evaluate differences among various batches and reaction conditions. Unfortunately, conversion or number of repeating units is impossible to assess from the aromatic region where all peaks overlap. However, the width of the peaks, absence of terminus protons are empirical indicators of degree of polymerization and hence molecular weight. A further complication is that amide peaks which appear between 10 and 11 ppm are close to the D₂SO₄ peak, the H-bond with sulfuric acid which broadens both peaks, and it makes it challenging to decouple one from the other. All samples were relatively dilute; otherwise, the solution could not be pipetted into the 3 mm special tube required for D₂SO₄ NMR. Analogues were grouped as highlighted in Table 2, by structure, to assess the spectral differences of like

Table 2. Solubility and Molecular Weight Data via Size Exclusion Chromatography^a

polymer	solubility	$\bar{M}_{n,app}$ (kg/mol)	$\bar{M}_{w,app}$ (kg/mol)	D_M
P1	yes	3.76	4.52	1.49
P2	yes	4.60	7.03	1.53
P3	partial*	8.10	21.7	2.68
P4	yes	8.44	19.7	2.33
P11	partial*	5.41	10.7	1.98
P5	partial**	—	—	—
P7	partial**	—	—	—
P12	yes	11.1	20.4	1.84
P6	yes	30.7	66.3	2.15
P8	yes	35.5	81.8	2.3
P9	yes	35.6	78.9	2.2
P10	no	—	—	—
P13	yes	12.5	28.5	2.3
P14	yes	21.7	57.1	2.6
P15	yes	10.6	28.7	2.7

^aApparent molecular weight measured by SEC; D_M is the dispersity index and is calculated as the ratio of weight average by number-average molecular weight. *Presumably high molecular weight fraction of the polymer was not dissolved, so these compounds likely have an underestimated molecular weight; ** these compounds were soluble with heating, but they could not be detected by a RI detector. The only potential explanation is a match of refractive index with the GPC solution, which would make them undetectable.

polymers. All other polymers' NMRs can be found in the Supporting Information. Figure 2 illustrates polymers P1–P4 and P11. Compounds P1 and P2 were prepared via the Higashi method and, as we suspected by the early precipitation of the product from the reaction mixture, they appear to have a lower molecular weight. That is evident by the defined splitting of peaks in the aromatic region; the concentration of the analogues is roughly the same, so the width of the peaks is likely due to the increased number of repeating units and not concentration. Furthermore, compound P1 appears to be an oligomeric species, where the terminal terephthalic unit appears at ~8.2 ppm and the protonated terminal amine appears at ~7.2 ppm (due to sulfuric acid NMR solvent). The

internal PDA groups appear at ~7.7 ppm. Based on the rough integration of the overlapped peaks, it appears that there are four repeating units in the molecule (four TPAs and four PDAs), which is the only analogue where such assessments can be made. Although polymer P2 displays broader peaks than P1, it appears that this analogue also has a low molecular weight, perhaps slightly higher than P1. Analogues P3, P4, and P11 appear to have similar spectra, with P3 displaying the broadest peaks. Another difficulty encountered in analyzing the spectra is the interaction of the solvent (D₂SO₄) with terminal amine groups, and likely with amide groups within the polymer chain; this constant proton exchange results in the broadening and shifting of the solvent peak, adding to the complex problem of peak overlap. This is perfectly illustrated by the NMR of a terephthalic amide small molecule, Figure S16 in the Supporting Information, where unexpectedly, all peaks appear as doublets. This small compound was available in our lab and fully characterized by conventional NMR, so there is no doubt about its purity. The molecule has two amide groups, and the spectra indicate that part of the molecule is protonated, thereby causing a shift in all protons. Further, the amide group appears between 10 and 10.5 ppm, but when in D₂SO₄, the "solvent" peak undergoes splitting. As expected, in a polymer, these effects are magnified.

Analogues P6, P8, and P12 are all polymers containing *m*-PDA as the amine, prepared at room temperature (P6 and P8) or 0 °C conditions (P12). Their stacked spectra are shown in Figure 3.

While P6 and P8 exhibit a somewhat similar pattern, P12 looks distinctively different, with a broad peak at around 8.4 ppm. The *meta*-PDA analogue has a more complex structure, with overlapping aromatic peaks from the amine. It is unclear whether the broad double peaks in P12 are due to tuning or a proton exchange as shown for a small molecule (Figure S16). In all analogues, terminal *m*-PDA aromatic peaks are not detected as they would appear far up-field around 6 ppm, further substantiating full protonation of the amine in highly acidic media.

The next set of spectra examines analogues containing piperazine as the diamine, where both compounds were prepared via identical methods, P5 and P7, whose NMRs are shown in Figure 4. The piperazine compound has perhaps the least complicated spectra and peaks from TPA versus the amine are far resolved. If we presume that the small peaks downfield from the main broad peak at around 7.5 ppm belong to a terminal TPA unit, a simple integration indicates that there are 11 internal repeating units and 1 terminal unit, for a total of 12 repeating units. Both spectra from P5 and P7 corroborate this number. Similarly, this analogue is expected to have protonated terminal amines, as well as undergo proton exchange via internal amide bonds in a strong acidic medium such as sulfuric acid.

3.5. Molecular Weight Evaluation. As previously mentioned, aramid polymers are generally not characterized via GPC due to their stark insolubility in all organic solvents, with few reported exceptions.^{10,24,32–35} The soluble compounds typically require laborious syntheses to prepare monomers that impart some solubility to the aramid product in organic solvents. We were delighted to find an additive that provided partial or full solubility at 3 mg/mL of most of our polymeric analogues, which enabled GPC-SEC characterization of at least some of our polymers. Table 2 summarizes the solubility of the polymers in the additized NMP, and where

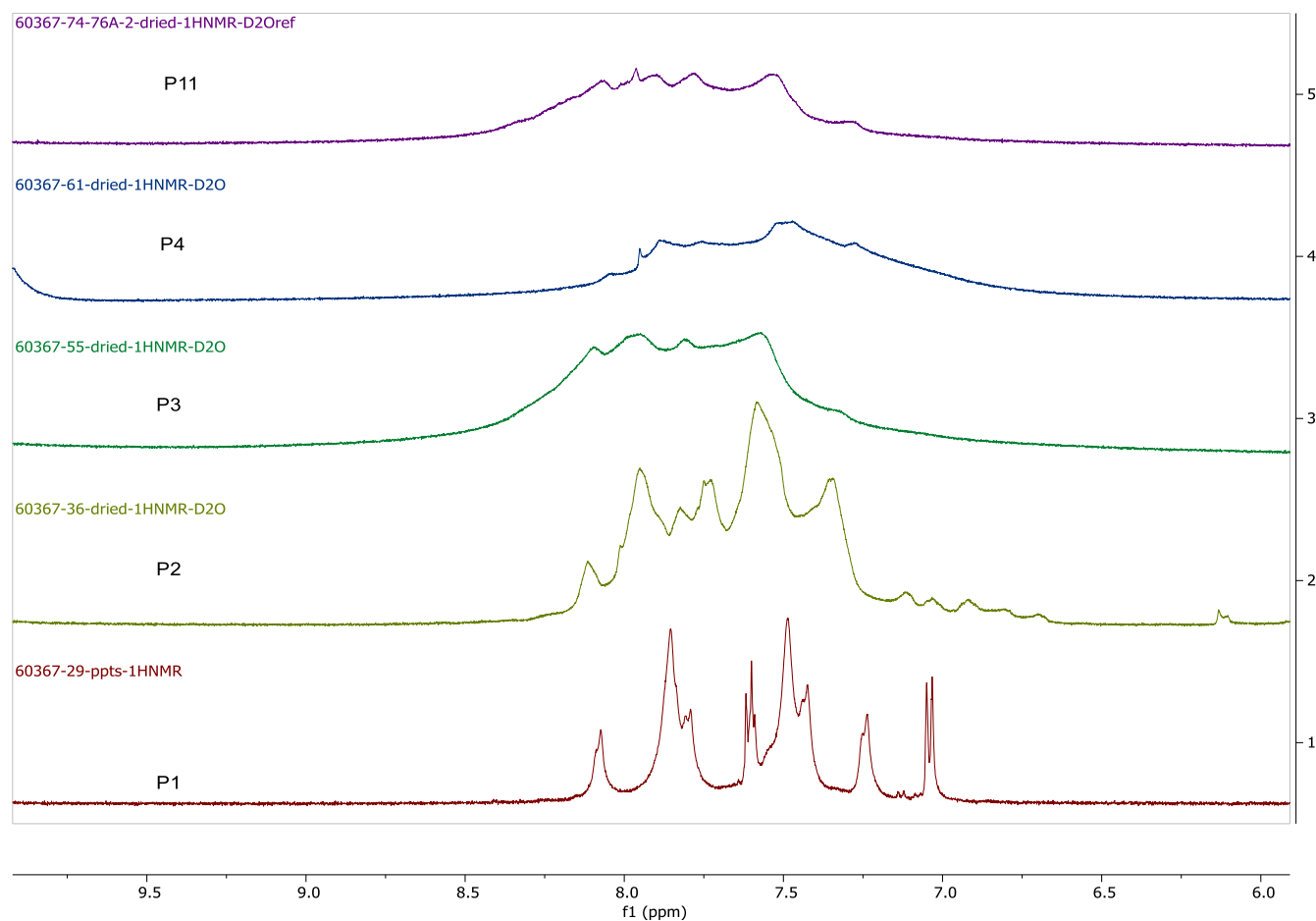


Figure 2. ^1H NMR of **P1**, **P2**, **P3**, **P4**, and **P11** in D_2SO_4 .

appropriate, their respective measured apparent molecular weights. Notably, **P8** and **P9** have the highest apparent molecular weights. The cause of this enhanced molecular weight can be twofold: either the enhanced solubility promoted the reaction further while preventing the early precipitation of low molecular weight polymers; or the prior filtration of the GPC sample before injection removed higher molecular weight fractions from the less soluble polymers, while the more soluble ones always remained in the solution. Efforts are underway to dissolve the polymers that were partially solvated in the NMP solution.

GPC confirmed the spectroscopic findings in that **P1** and **P2** were low molecular weight polymers. Interestingly, **P5** and **P7**, the piperazine-based polymers, were not detected by the RI detector, despite their dissolution in the solvent system. Interestingly, the *meta*-PDA series shows that the room-temperature analogues (**P6** and **P8**) have substantially higher molecular weight than the polymer prepared at $0\text{ }^\circ\text{C}$ (**P12**). It is difficult to assess whether the same is true for the *para*-PDA compounds since their molecular weight is underestimated due to limited solubility, as indicated in Table 2. Intrigued by these findings that contradict the general accepted protocol for these materials syntheses ($0\text{ }^\circ\text{C}$, in the presence of $\sim 5\%$ LiCl or CaCl_2), we examined the molecular weights of the **P9** analogue prepared under various conditions (Table 3) against polystyrene GPC standards.

P9 was chosen for this study because of its full solvation in the GPC solvent, leading therefore to a more accurate

estimation of its molecular weight. The starting material concentration was the same for all runs. Our data shows that RT, without CaCl_2 , yields the highest molecular weight polymer, followed by $0\text{ }^\circ\text{C}$ without CaCl_2 . In the presence of CaCl_2 , the temperature does not appear to have an effect, the molecular weight being presumably governed by CaCl_2 . All polycondensations led to a thickening of the NMP reaction mixture, without precipitation of the product. Future work and scale-up will focus on those polymers with highest molecular weight since it is the main driver in the strength of the subsequently formed fibers.

3.6. Thermal Analysis. The isolated bulk powders/polymers were analyzed via TGA and DSC to evaluate their decomposition onset, identify the relative differences among analogues with the same structures prepared via various conditions, and determine their melting points or glass-transition temperatures (T_g). The maximum temperature the sample was subjected to for TGA analysis was $700\text{ }^\circ\text{C}$. We suspected that all meaningful thermal events would occur well before this temperature. Similarly, DSC was only run up to $300\text{ }^\circ\text{C}$, well above the temperature where any application employing these polymers would take place. All DSCs are reported in the Supporting Information. Unsurprisingly, the bulk powders did not display a T_g or a liquid crystalline phase, which is of no consequence since the polymers will be processed from sulfuric acid. The liquid crystalline phase (nematic) is obtained when the polymer is dissolved in sulfuric acid and then shear enables molecular alignment and renders

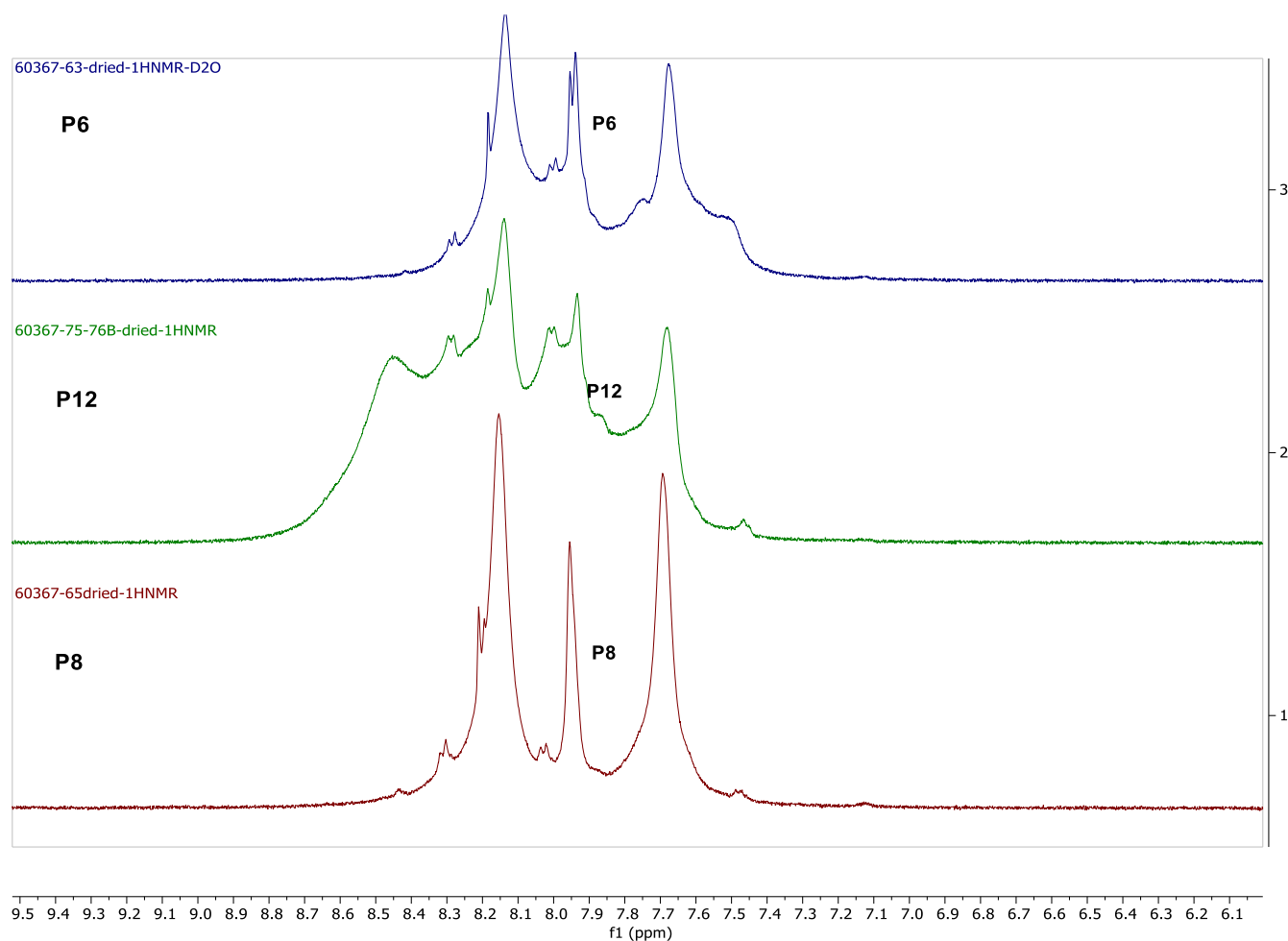


Figure 3. ^1H NMR of P6, P8, and P12 in D_2SO_4 .

strength to the fiber. Table 4 summarizes the decomposition temperature at 5% weight loss, 10% weight loss, and char yield at 700 °C. It is important to note that solid samples were not dried above room temperature prior to TGA analysis; however, DSCs were conducted on dried samples, after drying at 90 °C for 4 h under vacuum. Therefore, in many samples, a low-temperature weight loss of 3–6% is observed by TGA, below 125 °C, which is not an effect of materials' thermal or oxidative stability. Furthermore, TGAs shown below were run in air, which would further enhance the oxidative decomposition events.

The TGA data generally shows a high thermal stability, as expected from aramid polymers, with high percent char values, indicative of a high thermal stability of up to 700 °C. Most of the materials have not reached a char state per the definition of char and still appeared as the original solids, slightly colored. The best way to evaluate the data is to compare the same polymers prepared via different conditions (see Table 1) since one of the goals of this work was to identify the simplest, most efficient pathways to aramids and not obtaining the highest stability polymer. Therefore, the polymers were grouped and highlighted (gray or yellow) based on composition, with several not having a direct comparison. Polymers P1–P4 and P11 are condensation polymers containing *p*-PDA, the most linear, just like Kevlar, and are plotted in Figure 5a. P1 and P2 were prepared via the Higashi method utilizing anhydrous reagents and Schlenk techniques, without further drying and

distilling reagents. Compounds P1 and P2 are similar spectroscopically, likely both oligomers, with P1 having fewer repeating units than P2. P1 displays a higher char value and similar $T_{10\%}$ to P2. The gradual weight loss up to $T_{10\%}$ of P2 suggests the presence of starting materials undergoing sublimation, particularly TPA which starts subliming at ~180 °C and continues up to 300 °C. In contrast, the same composition polymers prepared via TPA chloride, P3, P4, and P11 are much more stable with $T_{10\%}$ values well over 500 °C. Compounds P3 and P4 were prepared via similar protocols at room temperature and no additives, while analogue P11 was prepared in the presence of CaCl_2 at 0 °C. Although P11 $T_{5\%}$ is very low, we believe that it is due to a water/NMP content and mass loss, not other chemical events, as $T_{10\%}$ is comparable to P3 and P4. P11 also displays a lower char content, consistent with higher decomposition rates.

Analogues P5 and P7 contain piperazine and were prepared via identical procedures, with P7 being a slight scale-up of P5. Both analogues display similar TGA profiles (Figure 5b), with a lower $T_{10\%}$, indicative of a lower thermal stability versus other analogues, and the lowest percent char among all compounds, indicative of severe bond cleavage and decomposition up to 700 °C. Piperazine not being aromatic, behaves more like a cyclohexane, with multiple conformations, preventing close packing of the polymer chains, and prone to thermal/oxidative cleavage. It is encouraging that both compounds display similar behaviors, only subtle differences likely due to inherent

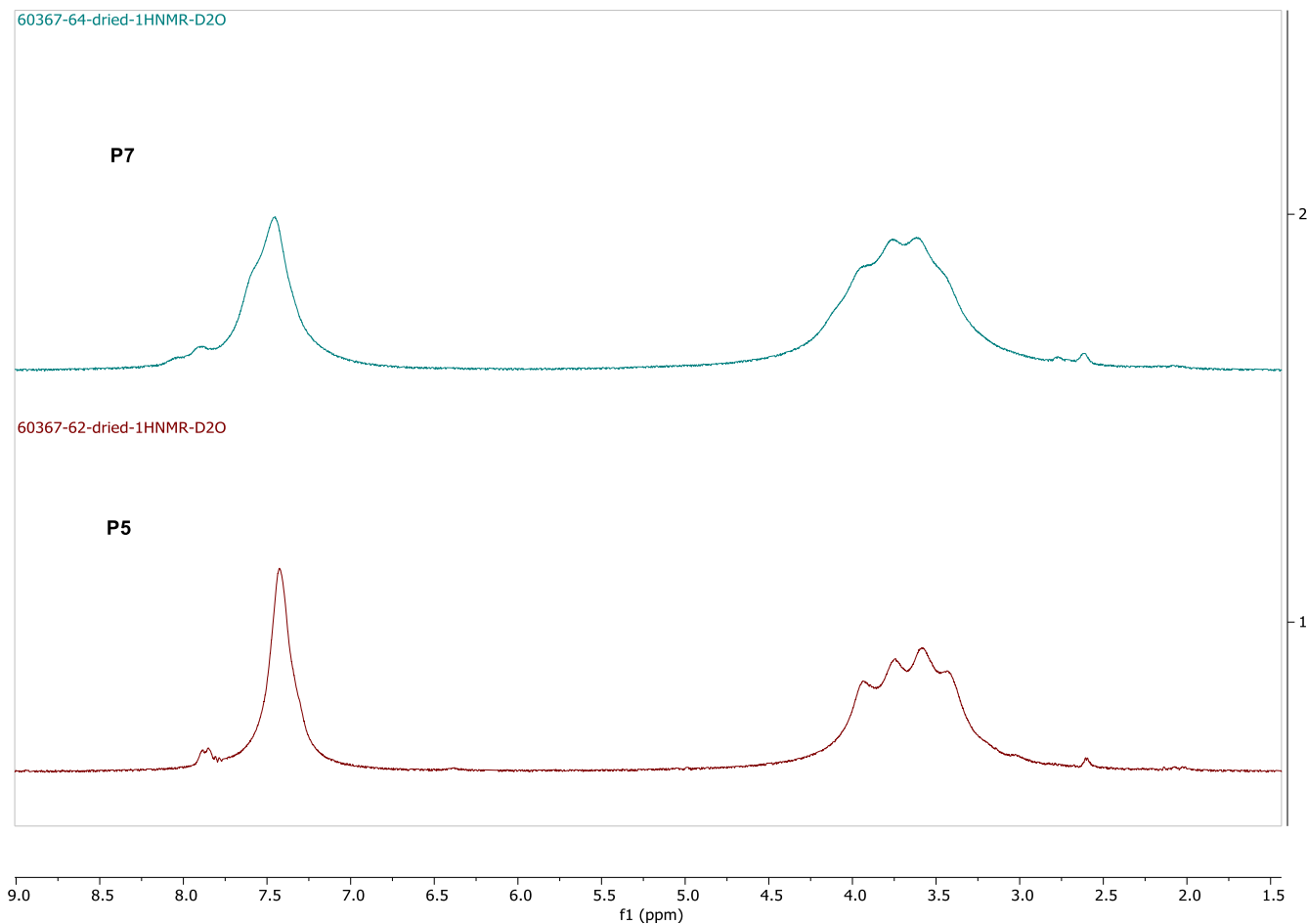


Figure 4. ^1H NMR of P5 and P7 in D_2SO_4 .

Table 3. Molecular Weight Dependency on Temperature and CaCl_2 ^a

polymer	conditions	$\bar{M}_{n,\text{app}}$ (kg/mol)	$\bar{M}_{w,\text{app}}$ (kg/mol)	D_M
P9	RT, no CaCl_2	37.3	62.0	1.66
P9-1	RT, CaCl_2	25.6	45.8	1.79
P9-2	0 °C, CaCl_2	24.7	42.3	1.70
P9-3	0 °C, no CaCl_2	29.7	53.3	1.79

^aThe molecular weights in Table 2 are evaluated against polymethacrylate standards, while these molecular weights are evaluated against polystyrene standards.

experimental errors. Piperazine does not appear like a promising candidate with respect to synthesis (nucleophilic amine that scavenges HCl) and thermal performance.

Analogues **P6**, **P8**, and **P12** are condensation polymers containing *meta*-PDA. The notable differences in this series is that **P6** and **P8** only differ in the concentration reaction mixture that generated them, with **P6** being lower concentration, ran without additives at RT, while **P12** was prepared in a solution containing CaCl_2 at 0 °C. Surprisingly, **P6** and **P8** have different thermal profiles shown in Figure 5c, with **P6** displaying weight loss early, inconsistent with just solvent loss, but rather the presence of subliming starting materials from an incomplete reaction, or decomposition of oligomeric small fragments. **P8** remains stable up to ~460 °C, after a very early solvent or intrinsic water loss. The percent char appears different in both analogues most likely due to an instrument

Table 4. Thermal Stability Data of All Polymer Analogues from TGA under Air Conditions

polymer	$T_{5\%}$ (°C)	$T_{10\%}$ (°C)	% char/residue yield
P1	186	488	50
P2	260	462	26
P3	494	530	35
P4	503	526	45
P11	508	540	26
P5	358	383	10
P7	394	416	12
P12	417	503	27
P6	162	461	52
P8	463	499	60
P9	479	511	42
P10	477	499	26
P13	125	518	45
P14	501	531	39
P15	489	497	52

artifact. The cold temperature synthesis yielded a more thermally stable compound—**P12**, similar to **P8**, suggesting that the differing reaction conditions did not affect the polymer properties.

P9, **P10**, and **P15** are condensation polymers of TPA chloride with a single amine, ODA, NapDA, and DADPM, respectively. One of the reasons for preparing ODA and DADPM homopolymers was to increase the solubility, with

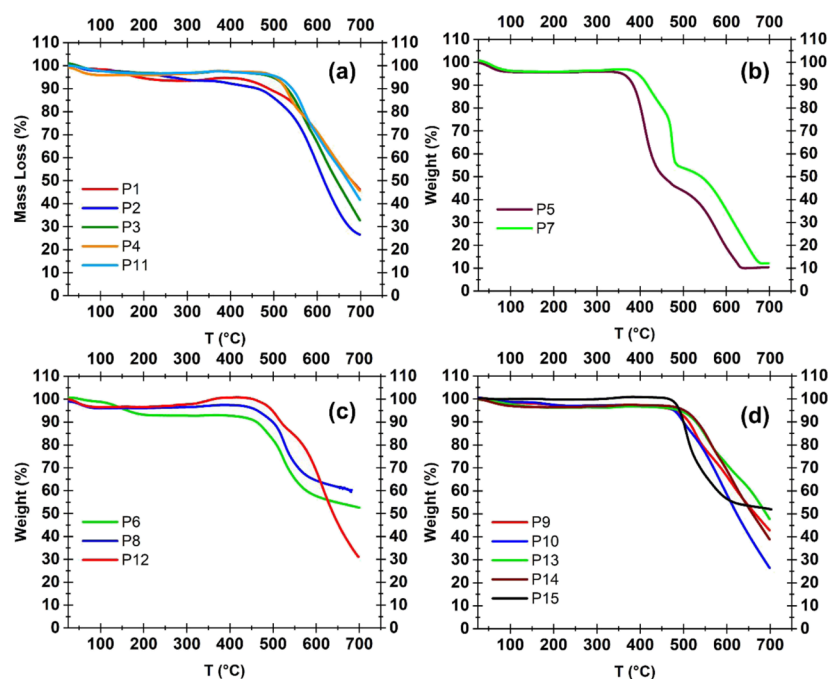


Figure 5. Percent mass loss as a function of temperature obtained for different synthesized polymers: (a) P1–P4 and P11. (b) P5 and P7. (c) P12, P6, and P8. (d) P9, P10, P13, P14, and P15.

the expectation of a thermal stability tradeoff versus the *para*-PDA. Their TGA plots are displayed in Figure 5d. Surprisingly, the ODA analogue, P9, has a very high thermal stability despite the weaker C–O bond present in the backbone, and less than linear structure, just as the Nap-DA analogue P10. They both have similar $T_{5\%}$ and $T_{10\%}$, while P9 appears more stable up to 700 °C, with a higher percent char (42 vs. 52%). P13 and P14 are co-polymers prepared with two amines in various molar ratios (see Table 1) with the aim of altering the recalcitrant poor solubility of the Kevlar-like polymer prepared with *para*-PDA. Since P9 was the most soluble analogue, copolymers with their respective oxygenated amine ODAs were prepared (P13 and P14). P13 has a low $T_{5\%}$, most likely due to the solvent trapped in the solid at 125 °C but has a high $T_{10\%}$ at 518 °C, consistent with the rest of the analogues. P14 has a high $T_{5\%}$ at 501 °C and a $T_{10\%}$ at 531 °C. The slightly higher ODDA content of P13 versus P14 (25% versus 10%) does not appear to significantly influence the thermal stability; both analogues have high percent char yields at 700 °C, which support high thermal stability.

All compounds were also analyzed by TGA under N₂, to avoid early oxidative events occurring under air, and those TGAs can be found in the Supporting Information. Although most polymers displayed a similar char percentage under N₂, in the absence of air, there are no intermediate “transition” events likely seen due to high-temperature oxidation reactions. In addition, the slightly increased weight % observed for samples analyzed by TGA under N₂ is presumably due to an artifact of the instrument rather than an increase in the sample mass of the polymer studied.

4. CONCLUSIONS

The present work demonstrates a sustainable strategy to Kevlar-like aramid polymers from waste PET, including mixed-waste PET. A series of aramid polymers were synthesized from the PET depolymerization monomer, TPA, via a simple and

economically viable route. We described various synthetic approaches and challenges encountered with them, which have led to the traditional route to prepare such polymers. Direct depolymerization of PET with aliphatic diamines under melt conditions resulted mainly in decomposition without substantial formation of any aramid polymer. The Higashi–Ogata methodology, direct polycondensation of TPA and *para*-PDA resulted in oligomerization and formation of aramids with low degree of polymerization. Although we aimed to bypass the less desirable reagents to prepare the acid chloride, ultimately, TPA was converted to the much more reactive species via thionyl chloride treatment, in quantitative yield. The highest molecular weight polymers, as determined spectroscopically and subsequently via GPC-SEC, were obtained via the acid chloride of TPA. Although a well-established method, polycondensation via acid chloride and diamine is both a science and an art. We investigated several conditions to improve the conversion but more importantly prevent the product from precipitating out and essentially reducing the molecular weight of the final polymer. We found that pyridine (2 eq) addition to the NMP reaction medium to neutralize the HCl generated also prevented the precipitation of the polymer. While reactions ran at 0 °C led to the formation of a gel, at room temperature, they led to only a slight thickening of the NMP solutions. The GPC of soluble analogues indicates that higher molecular weights are obtained at higher temperatures. Current work will probe this finding. Neither temperature led to the precipitation of the polymer (with few exceptions) which may be an important attribute, if future processing of these materials into fibers is attempted from crude reaction mixtures for additional cost benefits. A proprietary solvent composed of NMP and a 3–5% organic additive enabled the dissolution of nearly all polymers and subsequent GPC analysis in the same solvent system. The apparent molecular weights of the soluble polymer ranged between 10–35 kDa (M_n) and 28–81 kDa (M_w), values which are comparable or better than

other reported literature (referenced earlier). All analogues had high degradation temperatures at 5% and 10% weight loss ($T_{5\%}$ and $T_{10\%}$), above 400 °C, along with high percent char values. A glass transition (T_g) was not detected in any of the powder analogues prepared. To our knowledge, this is the first example of aramid polymers derived from waste plastics, such as PET. Notably, as reported in previous work, the nature of the waste PET (mixed, clean) does not affect the purity of the derived TPA and efficiency of the subsequent polycondensation. Future work will focus on scale-up of high molecular weight polymers, evaluation of their viscosity at various concentrations in sulfuric acid to determine optimal concentration for fiber spinning, and finally characterize the fibers obtained from various processing conditions.

■ ASSOCIATED CONTENT

SI Supporting Information

The Supporting Information is available free of charge at <https://pubs.acs.org/doi/10.1021/acsomega.2c03059>.

¹HNMR spectra of all polymers and several benchmarks, TGAs in air and N₂, DSC plots, and GPC calibration curve (PDF)

■ AUTHOR INFORMATION

Corresponding Author

Lelia Cosimbescu – Pacific Northwest National Laboratory, Richland, Washington 99354, USA; orcid.org/0000-0003-3055-4867; Email: lelia.cosimbescu@eastman.com

Authors

Deepika Malhotra – Pacific Northwest National Laboratory, Richland, Washington 99354, USA; orcid.org/0000-0002-0796-6508

Madhusudhan R. Pallaka – Pacific Northwest National Laboratory, Richland, Washington 99354, USA

Marie S. Swita – Pacific Northwest National Laboratory, Richland, Washington 99354, USA

Complete contact information is available at: <https://pubs.acs.org/doi/10.1021/acsomega.2c03059>

Author Contributions

L.C. proposed the study, directed the synthesis, analyzed the results, and coordinated the collaborations. D.M. conducted the synthesis and analyzed the results. M.R.P. conducted DSC and TGA experiments and analyzed the results. M.S. conducted GPC measurements and analyzed the results. All authors wrote and reviewed this manuscript.

Notes

The authors declare no competing financial interest.

■ ACKNOWLEDGMENTS

The research was supported by the U.S. Department of Energy (DOE), Vehicle Technology Office (VTO), VT1700000-05450-1005701, agreement # 36934. The views expressed in the article do not necessarily represent the views of the U.S. Department of Energy or the United States Government. The authors gratefully acknowledge the support and guidance of Dr. Felix Wu, DOE. The authors are also grateful to Cortland Johnson (PNNL) for improving the TOC image.

■ REFERENCES

- (1) Plastics Europe. "Plastics—the Facts 2020", Association of Plastic Manufacturers, 2020.
- (2) Vollmer, I.; Jenks, M. J. F.; Roelands, C. P.; White, R. J.; Harmelen, T.; Wild, P.; Laan, G. P.; Meirer, F.; Keurentjes, J. T. F.; Weckhuysen, B. M. Beyond Mechanical Recycling: Giving New Life to Plastic Waste. *Angew. Chem., Int. Ed. Engl.* **2020**, *59*, 15402–15423.
- (3) The Business Research Company *Polyethylene Terephthalate Global Market Report Summary 2020*, p 2020.
- (4) Barnard, E.; Rubio Arias, J. J.; Thielemans, W. Chemolytic depolymerisation of PET: a review. *Green Chem.* **2021**, *23*, 3765–3789.
- (5) Chawla, K. K. Chapter 4: Synthetic polymeric fibers" in *Fibrous Materials*; Cambridge University Press, 2016, pp 69–113: Cambridge.
- (6) DuPont, *Kevlar Technical Guide*, 2017, p 5.
- (7) Jingsheng, B.; Anji, Y.; Shengqing, Z.; Shufan, Z.; Chang, H. Studies on the Semirigid Chain Polyamide-Poly(1,4-Phenyleneter-ephthalamide). *J. Appl. Polym. Sci.* **1981**, *26*, 1211–1220.
- (8) Singh, T. J.; Samanta, S. Characterization of Kevlar fiber and its composites: a review. *Mater. Today: Proc.* **2015**, *2*, 1381–1387.
- (9) Cosimbescu, L.; Merkel, D. R.; Darsell, J.; Petrossian, G. Simple But Tricky: Investigations of Terephthalic Acid Purity Obtained from Mixed PET Waste. *Ind. Eng. Chem. Res.* **2021**, *60*, 12792–12797.
- (10) Merkel, D. R.; Kuang, W.; Malhotra, D.; Petrossian, G.; Zhong, L.; Simmons, K. L.; Zhang, J.; Cosimbescu, L. Waste PET chemical processing to terephthalic amides and their effect on asphalt performance. *ACS Sustainable Chem. Eng.* **2020**, *8*, 5615–5625.
- (11) Kudo, K.; Suguie, T.; Hiram, M. Melt-polymerized aliphatic-aromatic copolyamides. I. Melting points of nylon 66 copolymerized with aromatic diamines and terephthalic acid. *J. Appl. Polym. Sci.* **1992**, *44*, 1625–1629.
- (12) Wang, W. Z.; Zhang, Y. H. Environment-friendly synthesis of long chain semiaromatic polyamides. *eXPRESS Polym. Lett.* **2009**, *3*, 470–476.
- (13) Chen, Y. H.; Ranganathan, P.; Lee, Y. H.; Rwei, S. P. New Strategy and Polymer Design to Synthesize Polyamide 66 (PA66) Copolymers with Aromatic Moieties from Recycled PET (rPET). *ACS Sustainable Chem. Eng.* **2021**, *9*, 3518–3528.
- (14) Yamazaki, N.; Matsumoto, N.; Higashi, F. Studies on reactions of the N-phosphonium salts of pyridines. XIV. Wholly aromatic polyamides by the direct polycondensation reaction by using phosphites in the presence of metal salts. *J. Polym. Sci.* **1975**, *13*, 1373–1380.
- (15) Higashi, F.; Ogata, S.-I.; Aoki, Y. High-molecular-weight poly(p-phenyleneter-ephthalamide) by the direct polycondensation reaction with triphenyl phosphite. *J. Polym. Sci., Part A: Polym. Chem.* **1982**, *20*, 2081–2087.
- (16) García, J. M.; García, F. C.; Serna, F.; de la Peña, J. L. High-performance aromatic polyamides. *Prog. Polym. Sci.* **2010**, *35*, 623–686.
- (17) Reglero Ruiz, J. A.; Trigo-López, M.; García, F. C.; García, J. M. Functional aromatic polyamides. *Polymers* **2017**, *9*, 414.
- (18) Li, N.; Zhang, X. K.; Yu, J. R.; Wang, Y.; Zhu, J.; Hu, Z. M. Synthesis and characterization of easily colored meta-aramid copolymer containing ether bonds. *Chin. J. Polym. Sci.* **2019**, *37*, 227–234.
- (19) Liu, F. L.; He, J. J.; Yang, H. X.; Yang, S. Y. Improved Properties of Aromatic Polyamide Tape-casting Films. *Chin. J. Polym. Sci.* **2020**, *38*, 1345–1354.
- (20) Rapakousiou, A.; López-Moreno, A.; Nieto-Ortega, B.; Bernal, M. M.; Monclús, M. A.; Casado, S.; Navío, C.; González, L. R.; Fernández-Blázquez, J. P.; Vilatela, J. J.; Pérez, E. M. Stronger aramids through molecular design and nanoprocessing. *Polym. Chem.* **2020**, *11*, 1489–1495.
- (21) Yu, Z.; Deng, R.; Rao, G.; Lu, Y.; Wei, Y.; Fu, C.; Yan, X. F.; Cao, D.; Zhang, D. Synthesis and characterization of highly soluble wholly aromatic polyamides containing both furanyl and phenyl units. *J. Polym. Sci.* **2020**, *58*, 2140–2150.

(22) Ferrero, E.; Espeso, J. F.; de la Campa, J. G.; de Abajo, J.; Lozano, A. E. Synthesis and Characterization of Aromatic Polyamides Containing Alkylphthalimido Pendent Groups. *J. Polym. Sci., Part A: Polym. Chem.* **2002**, *40*, 3711–3724.

(23) Zhou, S.; Zhang, M. Y.; Wang, R.; Ping, J.; Zhang, X.; Zhao, N.; Xu, J.; Shen, Z. H.; Fan, X. H. Synthesis and characterization of new aramids based on o-(m-triphenyl)-terephthaloyl chloride and m-(m-triphenyl)-isophthaloyl chloride. *Polymer* **2017**, *109*, 49–57.

(24) Tamami, B.; Yeganeh, H. Synthesis and properties of novel aromatic polyamides based on 4-aryl-2,6-bis(4-chlorocarbonylphenyl)pyridines. *Eur. Polym. J.* **2002**, *38*, 933–940.

(25) Amininasab, S. M.; Rashidi, A.; Taghavi, M.; Shami, Z. Preparation and characterization of novel thermostable polyamides bearing different photoactive pendent architectures with antibacterial properties. *Chin. J. Polym. Sci.* **2016**, *34*, 766–776.

(26) Kusama, M.; Matsumoto, T.; Kurosaki, T. Soluble Polyimides with Polyalicyclic Structure.3. Polyimides from (4arH,8acH)-Decahydro-1t,4t:5c,8c-dimethanonaphthalene- 2t,3t,6c,7c-tetracarboxylic 2,3:6,7-Dianhydride. *Macromolecules* **1994**, *27*, 1117–1123.

(27) Cheng, L.; Jian, X. G. Synthesis of New Soluble Aromatic Poly(amide imide)s from Unsymmetrical Extended Diamine Containing Phthalazinone Moiety. *J. Appl. Polym. Sci.* **2004**, *92*, 1516–1520.

(28) Pal, R. R.; Patil, P. S.; Salunkhe, M. M.; Maldar, N. N.; Wadgaonkar, P. P. Synthesis, characterization and constitutional isomerism study of new aromatic polyamides containing pendant groups based on asymmetrically substituted meta-phenylene diamines. *Eur. Polym. J.* **2009**, *45*, 953–959.

(29) inventor; El Du Pont de Nemours and Co, assignee. Blades, H. Dry jet wet spinning process. U.S. Patent no 3767756 A, 1973 (Oct 23, 1973).

(30) Hancock, T. A. J. E.; Spruiell, J. L.; White, J. L. Wet spinning of aliphatic and aromatic polyamides. *J. Appl. Polym. Sci.* **1977**, *21*, 1227–1247.

(31) Yang, B.; Wang, L.; Zhang, M.; Luo, J. D. X.; Ding, X. Timesaving, high-efficiency approaches to fabricate aramid nanofibers. *ACS Nano* **2019**, *13*, 7886–7897.

(32) Oishi, Y.; Takado, H.; Yoneyama, M.; Kakimoto, M. A.; Imai, Y. Preparation and properties of new aromatic polyamides from 4, 4'-diaminotriphenylamine and aromatic dicarboxylic acids. *J. Polym. Sci., Part A: Polym. Chem.* **1990**, *28*, 1763–1769.

(33) Yang, C. P.; Oishi, Y.; Kakimoto, M. A.; Imai, Y. Preparation and properties of aromatic polyamides from 5-t-butylisophthalic acid and various aromatic diamines. *J. Polym. Sci., Part A: Polym. Chem.* **1989**, *27*, 3895–3901.

(34) Cao, K.; Liu, Y.; Yang, Y.; Yuan, F.; Wang, J.; Liu, H.; Jiang, M.; Yang, J. The preparation and characterization of a heterocyclic meta-aramid fiber with outstanding thermal stability. *High Perform. Polym.* **2020**, *33*, 554–567.

(35) Xu, R.; Qiu, Y. S.; Tang, C.; Yang, Y.; Dai, D.; Zhang, Y.; Gao, K.; Gao, L.; Luo, X.; Liu, X. Preparation of High Strength and Toughness Aramid Fiber by Introducing Flexible Asymmetric Monomer to Construct Misplaced-Nunchaku Structure. *Macromol. Mater. Eng.* **2021**, *306*, 2000814.